Prestack first-break traveltime tomography using the double-square-root eikonal equation

Siwei Li, Sergey Fomel, The University of Texas at Austin, and Alexander Vladimirsky, Cornell University*

SUMMARY

Traveltime tomography with shot-based eikonal equation fixes shot positions then relies on inversion to resolve any contradicting information between independent shots and achieve a possible cost-function minimum. On the other hand, the double-square-root (DSR) eikonal equation that describes the whole survey, while providing the same first-arrival traveltimes, allows not only the receivers but also the shots to change position and therefore leads to faster convergence in tomographic inversion. The DSR eikonal equation can be solved by a version of the fast-marching method (FMM) with special treatment for its singularity at horizontally traveling waves. For inversion, we use an upwind finite-difference scheme and the adjoint-state method to avoid explicit calculation of Fréchet derivatives. The proposed method generalizes to the 3D case straightforwardly.

INTRODUCTION

First-arrival traveltime tomography has been an established geophysical tool for estimating macro-feature seismic velocities in the near surface (Osypov, 2000; Leung and Qian, 2006; Taillandier et al., 2009; Noble et al., 2010). The traditional traveltime tomography uses so-called eikonal equation that comes from the leading-order WKBJ approximation of the wave equation (Bleistein, 2001; Chapman, 2002). The eikonal equation can be solved by various numerical methods, with ray-tracing (Zhu et al., 1992), fast-marching method (Sethian, 1999) and fast-sweeping method (Zhao, 2005) as some of the most popular choices. For each shot, the forward eikonal solver considers only the propagating wave-front as it gradually reaches receivers further away from the fixed source. It mimics the field acquisition process where we release one shot at a time. At inversion, the standard least-squares minimization cost-function sums over data misfits at each source-receiver pair. The steepest-descent gradient out of this formulation collects back-projected data-misfit along each source-receiver trajectory (Sei and Symes, 1994; Taillandier et al., 2009). Since the problem is non-linear, several iterations may be required until convergence.

Because the traditional traveltime tomography relies on shot-indexed eikonal equations, we expect the inversion to resolve possible conflicting information in the data that happen across different shots. In other words, the forward modeling step disregards information flowing along shot dimension because the source position is always fixed. For this reason, the inversion may take more iterations to converge, compared to the situation where we find a way to describe the survey as a whole and also to allow shot positions to change in the governing equation. For the later case, the double-square-root (DSR) eikonal is appropriate. It links the vertical slowness to non-coincident source and receiver horizontal coordinates through a dispersion relation. Previous works (Iversen, 2004; Duchkov and de Hoop, 2009; Alkhalifah, 2011) solve DSR by extrapolating isochron rays and using perturbation theory. However, for tomography purposes, we are only interested in first-arrivals, and in this regard those methods are not cost-effective. Our analysis shows the causality of DSR makes it possible for it to be solved by a Dijkstra-like non-iterative method, leading to the unique viscosity, i.e. first-arrival, solution. Consequently, the velocity estimation through DSR tomography becomes feasible.

In the following sections, we will first briefly review the DSR eikonal equation, then solve it numerically with a version of the fast-marching method, and finally introduce a new tomographic scheme based on linearization.

THEORY

DSR and its FMM implementation

The DSR eikonal equation is a first-order PDE taking the following form (Belonosova and Alekseev, 1974):

$$\frac{\partial T}{\partial z} = \pm\sqrt{\frac{1}{v^2(s,z)} - \left(\frac{\partial T}{\partial s}\right)^2} \pm \sqrt{\frac{1}{v^2(r,z)} - \left(\frac{\partial T}{\partial r}\right)^2}, \quad (1)$$

where $v(x,z)$ is the velocity of the medium, $T(s,r,z)$ is the prestack traveltime, (s,z) and (r,z) are source and receiver locations respectively. The $\pm$ sign before square-roots arises from the ambiguity between ray-paths bending upward or downward. For simplicity, we restrict the analysis to 2D case in this paper. The 3D generalization is straight-forward. Equation (1) is known to have a singularity at horizontally traveling waves (Alkhalifah, 2011). By setting $\partial T/\partial z = 0$, equation (1) leads to two traditional eikonal equations:

$$\begin{cases} (\partial T/\partial s)^2 = 1/v^2(s,z), \\ (\partial T/\partial r)^2 = 1/v^2(r,z). \end{cases} \quad (2)$$

These two equations are in no conflict because they describe source-receiver reciprocity in continuum space (as an exchange of s and r provides the same set of equations). Iversen (2004) and Duchkov and de Hoop (2009) develop a ray-tracing treatment for (1) that allows them to control angles and avoid (2). Alkhalifah (2011) uses perturbation theory to expand solution of (1) for reflected waves in scattering angle and dip angle. These methods are either expensive or inaccurate. In fact, we can show that a semi-Lagrangian discretization of (1) follows causality, meaning the traveltime of currently considered grid point relies only on its upwind neighbors (Vladimirsky, 2008).

DOI http://dx.doi.org/10.1190/segam2012-0773.1

The proof also applies to a Eulerian discretization via Kuhn-Tucker optimality conditions. A Dijkstra-like non-iterative method, analogous to FMM, is thus applicable to DSR.

The local update equation for traditional eikonal reads

$$\left(\frac{\partial T}{\partial x}\right)^2 + \left(\frac{\partial T}{\partial z}\right)^2 = S^2. \tag{3}$$

After discretization and choosing of upwind neighbors, equation (3) represents a quadratic function of T. For DSR, the corresponding update can be obtained by either a root-search algorithm such as Newton's method or interval method based on (1) or an analytical evaluation. Denote $T_i = \partial T/\partial i, i = z,r,s$ and $W_s = 1/v^2(s,z)$, $W_r = 1/v^2(r,z)$, we cast (1) in a polynomial form in terms of power of T derivatives:

$$\begin{aligned}(T_s^4 + T_r^4 + T_z^4) + 2(T_s^2T_r^2 - T_s^2T_z^2 - T_r^2T_z^2)\\ -2(W_sT_s^2 + W_rT_r^2 - W_sT_r^2 - W_rT_s^2 + W_sT_z^2 + W_rT_z^2)\\ +(W_s^2 + W_r^2 - 2W_sW_r)\\ = 0\end{aligned} \tag{4}$$

Notice W_s and W_r are independent. Also, the $\pm$ ambiguity in (1) disappears. The first, second and third rows in (4) are power of T to the fourth, second and zero orders respectively. One should further supply the one-sided finite-difference approximation for all T_i as (h_i grid spacing and T_0^i the upwind neighbor in i-th direction):

$$T_i = \frac{\partial T}{\partial i} = \frac{T - T_0^i}{h_i} \tag{5}$$

into (4). Solving equation (4) and (5 amounts to finding a characteristic which is confined in the simplex formed by the three upwind neighbors (see Figure 1). The resulting quartic equation has an analytical solution by Ferrari's method (Spiegel, 1968). We pick the smallest real root that satisfies causality.

Finally, for horizontally traveling wave where $T_z = 0$, we take the smaller of two results from (2)

$$T = \min\left(T_0^r + \frac{h_r}{v(r,z)},\ T_0^s + \frac{h_s}{v(s,z)}\right). \tag{6}$$

First-arrival tomography with linearized DSR

We follow the same principle as for traditional tomography with shot-indexed eikonal to derive a non-linear inversion scheme based on DSR. The essential step is to linearize DSR by writing W_s, W_r and T in (4) as some background plus perturbation ΔW_s, ΔW_r and ΔT. After neglecting second-order terms, we arrive at

$$a_z\Delta T_z + a_r\Delta T_r + a_s\Delta T_s = b_r\Delta W_r + b_s\Delta W_s, \tag{7}$$

where

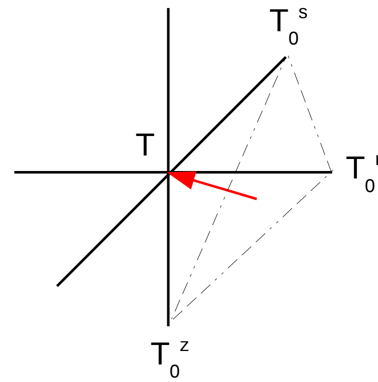

Figure 1: Local update through equation (4) and (5). T_0^z, T_0^r and T_0^s are chosen upwind neighbors, as follows from equation (5). The red arrow stands for the characteristic pointing towards to grid point to be updated. While the characteristic intersects the simplex at all possible angles, it should not be perpendicular to the z-direction due to singularity (2). DSR thus has an effective anisotropic behavior.

$$\begin{aligned} a_z &= 2T_z(T_z^2 + T_s^2 + T_r^2 - W_s - W_r),\\ a_r &= 2T_rb_r,\\ a_s &= 2T_sb_s,\\ b_r &= T_r^2 - T_s^2 + T_z^2 - W_r + W_s,\\ b_s &= T_s^2 - T_r^2 + T_z^2 - W_s + W_r.\end{aligned} \tag{8}$$

For the whole 2D discretized domain of size $nz \times nx$, system (7) can be written in a matrix-vector form as

$$\mathbf{A}\,\Delta T = \mathbf{B}\,\Delta W \tag{9}$$

While ΔW is a vector of length $nz \times nx$, ΔT is of size $nz \times nx \times nx$. The $\mathbf{A}$ contains characteristics of DSR eikonal, similar to the traditional tomography case. On the other hand, $\mathbf{B}$ is an operator that extends the 2D velocity model into 3D prestack volume because each grid point can be both source and receiver. We choose to obtain update ΔW by solving (9) in least-squares sense, i.e. we solve the following normal equation

$$\left[\mathbf{B}^t\,\mathbf{A}^{-t}\right]\left[\mathbf{A}^{-1}\,\mathbf{B}\right]\Delta W = \left[\mathbf{B}^t\,\mathbf{A}^{-t}\right]\Delta T \tag{10}$$

where superscript t stands for adjoint operator, and $-t$ stands for adjoint of the inverse.

Note that at singularity of DSR we should instead linearize (6). Following the same procedure above, we have

$$\Delta T_s = \frac{\Delta W_s}{2\sqrt{W_s}}\ \text{,or,}\ \Delta T_r = \frac{\Delta W_r}{2\sqrt{W_r}}. \tag{11}$$

and they can be easily incorporated into (7) so as to keep the same structure for (9). For example, if update (6) comes from source side, then

DOI http://dx.doi.org/10.1190/segam2012-0773.1

$$
\begin{aligned}
a_z &= 0, \\
a_r &= 0, \\
a_s &= 1, \\
b_r &= 0, \\
b_s &= 1/\left(2\sqrt{W_s}\right).
\end{aligned}
\tag{12}
$$

ALGORITHM

Our implementation is carried out in a regularly sampled Cartesian grid with spacing h_z and $h_s = h_r = h_x$ (for simplicity). Denote the discretized domain as $\underline{\Omega}$ with $\underline{x} \in \underline{\Omega}$ being grid points. Initial condition is defined on $\underline{\partial\Omega}$ with $T_0(\underline{x})$. Let $N(\underline{x})$ be the set of neighbors of node $\underline{x}$. A classic FMM algorithm makes use of a priority-queue (heap) structure and monotonically propagates wave-fronts:

---

foreach $\underline{x} \in \underline{\Omega}$ **do** $T(\underline{x}) \leftarrow \infty$
foreach $\underline{x} \in \underline{\partial\Omega}$ **do** $T(\underline{x}) \leftarrow T_0(\underline{x})$
$\Lambda \leftarrow \underline{\Omega} \cup \underline{\partial\Omega}$
while $\Lambda \neq \emptyset$ **do**
    $\underline{y} \leftarrow \mathit{ExtractMin}\,(\Lambda)$
    foreach $\underline{x_0} \in (N(\underline{y}) \cap \Lambda) \setminus \underline{\partial\Omega}$ **do** $T(\underline{x_0}) \leftarrow \mathit{Update}\,(\underline{x_0})$
end

For DSR, we modify function *Update* for (4) and (6). The computation can be restricted to $r - s \geq 0$ due to source-receiver reciprocity. Finally, $\underline{\partial\Omega}$ contains both $r = s$ with $T_0 = 0$ and $h_x = r - s$ with T_0 satisfying (6) (see Figure 2). If the total number of grid points is $n = nz \times nx \times nx$, then the computational complexity of FMM DSR is in order of $O\,(n\,log(n))$.

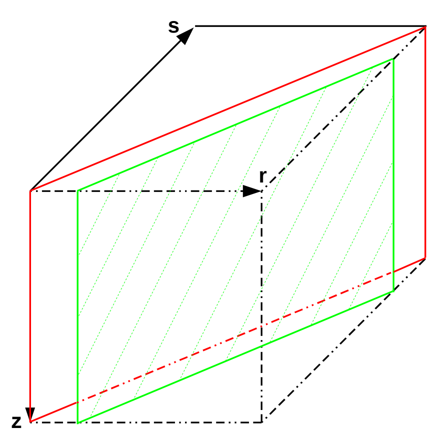

Figure 2: Schematic computational domain of FMM DSR eikonal. Zero-offset plane $r = s$ is indicated by red while grid points with $h_x = r - s$ are paint green. See text for more description on initialization and marching procedure.

We adopt the conjugate-gradient method (Hestenes and Stiefel, 1952) with Tickhonov regularization (Tarantola, 2004) to solve system (10). Tomography requires economical computation and, for this regard, **A** can be implemented efficiently by explicit upwind finite-difference scheme (Franklin and Harris, 2001), which results in $O(n)$ cost for applying forward or adjoint operators.

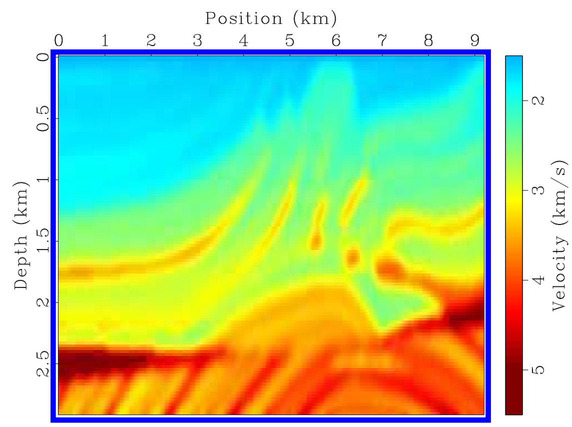

Figure 3: Smoothed Marmousi model. $nz = 384$, $nx = 122$, $dz = dx = 0.024$km.

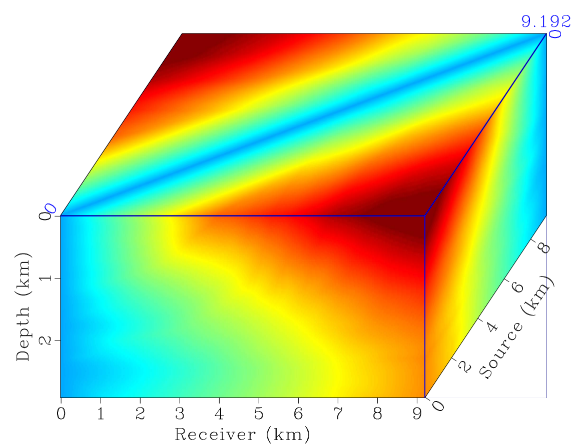

Figure 4: Prestack first-arrival traveltimes computed by FMM DSR. Compare with Figure 2.

SYNTHETIC EXAMPLES

We first demonstrate FMM DSR in a smoothed Marmousi model (Figure 3 and 4). Notice that generating the 3D volume through standard FMM requires at least solving half $nz \times nx$ eikonals, extracting depth slices and then concatenating results. If each eikonal solving is carried out by standard FMM, then the computational complexity is $O((nz \times nx)^2 \cdot log(nz \times nx))$. On the other hand, the cost of FMM DSR is of order $O((nz^2 \times nx) \cdot log(nz^2 \times nx))$.

To justify the accuracy of our method, we compare the results at three depth levels against those from a second-order FMM eikonal (Figure 5).

DOI http://dx.doi.org/10.1190/segam2012-0773.1

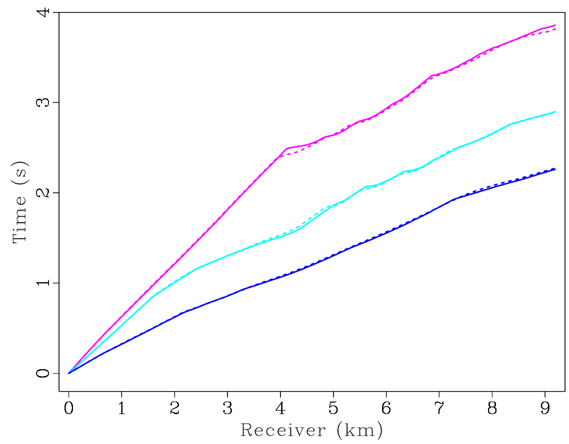

Figure 5: Comparison of results from second-order FMM Eikonal (solid line) and first-order FMM DSR (dashed line). Source locations from top to bottom: magenta $(0,0)$km; cyan $(0.96,0)$km; blue $(1.92,0)$km.

Next, we use a constant-velocity-gradient model as initial guess (Figure 6) and compute the first Gauss-Newton gradient from traditional tomography (Figure 7) as well as that from DSR tomography (Figure 8), both after 10 conjugate-gradient iterations and with the same Tickhonov regularization. The two gradients are different in both direction and length, with the one from DSR tomography providing more details that are suppressed in traditional tomography.

CONCLUSION AND DISCUSSION

In traditional shot-indexed eikonal tomography, the iterative inversion requires extra computations to resolve conflicting information from individual shots. A DSR-based first-arrival traveltime tomography can be advantageous because it considers prestack data as a whole. Due to causality of DSR, we show that it can be solved by FMM and a corresponding upwind finite-difference scheme is feasible for inversion.

DSR-based tomography shares the same fundamental drawbacks as traditional first-break tomography. For example, it can meet difficulty resolving velocity inversion. As an underdetermined non-linear problem, regularization is another critical component.

While our current implementation is for 2D velocity model, the extension to 3D is straightforward. While standard eikonal is shot-wise independent and thus parallelizable, FMM DSR is an essentially sequential algorithm. A parallel FMM DSR and field-data applications will be considered in future study.

ACKNOWLEDGMENTS

The work was supported by Saudi Aramco and KAUST. We thank Tariq Alkhalifah and Tim Keho for useful discussions.

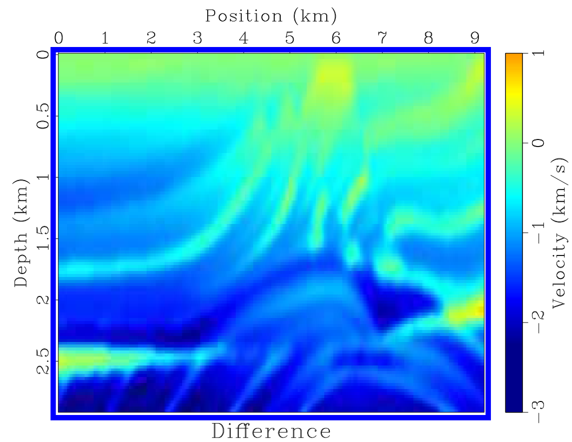

Figure 6: Difference between the smoothed Marmousi model and a constant-velocity-gradient initial model.

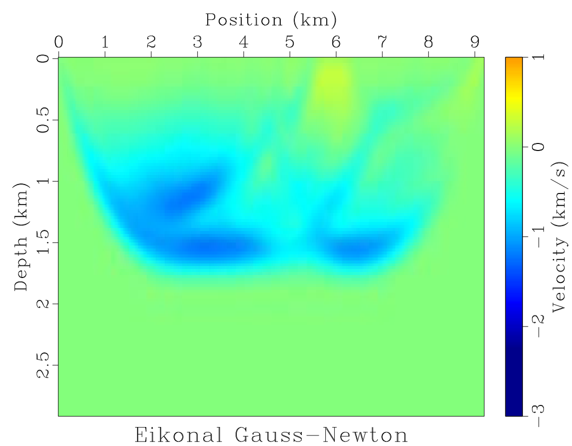

Figure 7: Gauss-Newton gradient from tomography with shot-indexed eikonal.

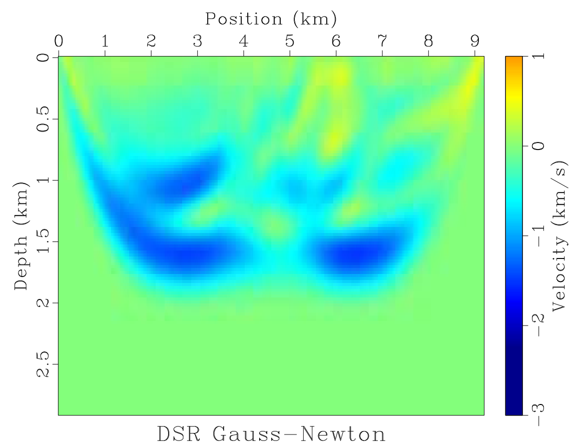

Figure 8: Gauss-Newton gradient from DSR tomography.

DOI http://dx.doi.org/10.1190/segam2012-0773.1

http://dx.doi.org/10.1190/segam2012-0773.1

EDITED REFERENCES

Note: This reference list is a copy-edited version of the reference list submitted by the author. Reference lists for the 2012 SEG Technical Program Expanded Abstracts have been copy edited so that references provided with the online metadata for each paper will achieve a high degree of linking to cited sources that appear on the Web.

REFERENCES

Alkhalifah, T., 2011, Prestack traveltime approximations: 81st Annual International Meetings, SEG, Expanded Abstracts, 3017–3021.

Belonosova, A. V., and A. S. Alekseev, 1974, About one formulation of the inverse kinematic problem of seismics for a two-dimensional continuously heterogeneous medium: Nauka.

Bleistein, N., 2001, Seismic ray theory: Cambridge University Press.

Chapman, C., 2002, Fundamentals of seismic wave propagation: Cambridge University Press.

Duchkov, A., and M. V. de Hoop, 2009, Extended isochron ray in prestack depth migration: 79th Annual International Meetings, SEG, Expanded Abstracts, 3610–3614.

Franklin, J. B., and J. M. Harris, 2001, A fast marching level set method for monotonically advancing fronts: Journal of Computational Acoustics, **9**, 1095–1109.

Hestenes, M. R., and E. Stiefel, 1952, Method of conjugate gradients for solving linear systems: Journal of Research of the National Bureau of Standards, **49**, 409–436.

Iversen, E., 2004, The isochron ray in seismic modeling and imaging: Geophysics, **69**, 1053–1070.

Leung, S., and J. Qian, 2006, An adjoint state method for three-dimensional transmission traveltime tomography using first arrivals: Communications in Mathematical Sciences, **4**, 249–266.

Noble, M., P. Thierry, C. Taillandier, and H. Calandra, 2010, High-performance 3D first-arrival traveltime tomography: The Leading Edge, **29**, 86–93.

Osypov, K., 2000, Robust refraction tomography: 70th Annual International Meetings, SEG, Expanded Abstracts, 2032–2035.

Sei, A., and W. Symes, 1994, Gradient calculation of the traveltime cost function without ray tracing: 64th Annual International Meetings, SEG, Expanded Abstracts, 1351–1354.

Sethian, J. A., 1999, Level set methods and fast marching methods: Evolving interfaces in computational geometry, fluid mechanics, computer vision and material sciences: Cambridge University Press.

Spiegel, M. R., 1968, Mathematical handbook of formulas and tables: Schaum.

Taillandier, C., M. Noble, H. Chauris, and H. Calandra, 2009, First-arrival traveltime tomography based on the adjoint-state method: Geophysics, **74**, no. 6, WCB1–WCB10.

Tarantola, A., 2004, Inverse problem theory and methods for model parameter estimation: SIAM.

Vladimirsky, A., 2008, Label-setting methods for multimode stochastic shortest path problems on graphs: Mathematics of Operations Research, **33**, 821–838.

Zhao, H., 2005, A fast sweeping method for Eikonal equations: Mathematics of Computation, **74**, 603–627.

Zhu, X., D. P. Sixta, and B. G. Angstman, 1992, Tomostatics: Turning-ray tomography + static corrections: The Leading Edge, **11**, 15–23.

DOI http://dx.doi.org/10.1190/segam2012-0773.1